LETTER

doi:10.1038/nature14213

Drought impact on forest carbon dynamics and fluxes in Amazonia

Christopher E. Doughty[1], D. B. Metcalfe[2], C. A. J. Girardin[1], F. Farfán Amézquita[3], D. Galiano Cabrera[3], W. Huaraca Huasco[3], J. E. Silva-Espejo[3], A. Araujo-Murakami[4], M. C. da Costa[5], W. Rocha[6], T. R. Feldpausch[7], A. L. M. Mendoza[3], A. C. L. da Costa[5], P. Meir[8,9], O. L. Phillips[10] & Y. Malhi[1]

In 2005 and 2010 the Amazon basin experienced two strong droughts[1], driven by shifts in the tropical hydrological regime[2] possibly associated with global climate change[3], as predicted by some global models[3]. Tree mortality increased after the 2005 drought[4], and regional atmospheric inversion modelling showed basin-wide decreases in CO_2 uptake in 2010 compared with 2011 (ref. 5). But the response of tropical forest carbon cycling to these droughts is not fully understood and there has been no detailed multi-site investigation *in situ*. Here we use several years of data from a network of thirteen 1-ha forest plots spread throughout South America, where each component of net primary production (NPP), autotrophic respiration and heterotrophic respiration is measured separately, to develop a better mechanistic understanding of the impact of the 2010 drought on the Amazon forest. We find that total NPP remained constant throughout the drought. However, towards the end of the drought, autotrophic respiration, especially in roots and stems, declined significantly compared with measurements in 2009 made in the absence of drought, with extended decreases in autotrophic respiration in the three driest plots. In the year after the drought, total NPP remained constant but the allocation of carbon shifted towards canopy NPP and away from fine-root NPP. Both leaf-level and plot-level measurements indicate that severe drought suppresses photosynthesis. Scaling these measurements to the entire Amazon basin with rainfall data, we estimate that drought suppressed Amazon-wide photosynthesis in 2010 by 0.38 petagrams of carbon (0.23–0.53 petagrams of carbon). Overall, we find that during this drought, instead of reducing total NPP, trees prioritized growth by reducing autotrophic respiration that was unrelated to growth. This suggests that trees decrease investment in tissue maintenance and defence, in line with eco-evolutionary theories that trees are competitively disadvantaged in the absence of growth[6]. We propose that weakened maintenance and defence investment may, in turn, cause the increase in post-drought tree mortality observed at our plots.

How does drought affect tropical forests? This question has been studied in long-term experimental drought studies[7,8], in long-term biomass plots that have tracked forest dynamics through drought events[4], and through remote sensing[9–11]. Increased mortality of trees in a large network of 1-ha plot censuses was observed after the 2005 Amazonian drought, turning the forest from an estimated net biomass carbon (C) sink of $\sim$0.71 Mg C ha^{-1} yr^{-1} (ref. 12) to a temporary net source of CO_2 to the atmosphere of twice this, with a total impact (that is, committed source minus baseline sink) of 1.2–1.6 Pg C (ref. 4). An increase in drought-induced tree mortality has also been seen in two multi-year experimentally droughted plots in Amazonia, dominated by an increase in the mortality of large trees[7]. Remote sensing of canopy backscatter after the 2005 drought indicated that, in some parts of Amazonia, the drought caused a change in structure and water content associated with the forest upper canopy. This suggests a slow recovery ($>$4 years) of forest canopy structure after the severe drought in 2005 (ref. 10).

Because future droughts in tropical regions may increase in frequency and severity[1–3], a better understanding of whether net CO_2 fluxes to the atmosphere from tropical forests increase or decrease during drought periods is urgently required. Drought could either suppress gross primary productivity (GPP), which would lead to an immediate decrease in CO_2 uptake, or it could decrease heterotrophic respiration, thereby decreasing the CO_2 source to the atmosphere, or both[13]. The Amazon basin in 2010 was drier than in 2011, but not warmer, permitting the influences of temperature and precipitation to be separated[5]. A recent atmospheric inversion study in the Amazon basin found that these forests took up 0.25 $\pm$ 0.14 Pg C less CO_2 in 2010 (the year of the drought) than in 2011, after accounting for the effect of increased fires during the drought[5]. A previous study using isotopic techniques found a similar result, with the basin turning from a potential sink to a source after the dry El Niño year of 1997 (ref. 14). These results indicate that annual Amazon droughts apparently suppress photosynthesis more than respiration, but such a relative decrease has not been directly verified with on-the-ground measurements.

To be able to understand and model long-term carbon storage in the tropics, top-down estimates of GPP and fluxes of CO_2 to the atmosphere alone are insufficient. It is also important to understand how the products of photosynthesis are allocated between plant metabolism and biomass growth (NPP) and how that growth is allocated among different organs of the tree[15]. Total autotrophic respiration plus total NPP should approximately equal total GPP over long (multi-year) timescales in a stable environment. However, over shorter timescales the two may differ, because forests may store 'old' carbon in the form of non-structural carbohydrates (NSCs), which may be abundant in tropical forests ($\sim$16 Mg C ha^{-1}, more than enough carbon to rebuild the entire leaf canopy)[16]. These NSCs may function as a reserve that enables the continuation of high rates of growth during periods of lower carbon income from photosynthesis[16–18].

For several years we have measured the main components of total NPP (including 1–3-month records of fine-root, woody and leaf-flush NPP) and autotrophic respiration (including rhizosphere, stem wood and canopy leaf respiration) at thirteen 1-ha rainforest plots in three South American countries, covering contrasting climatic and soil conditions and also across a 2,800 m elevation range in the Andes (Extended Data Tables 1–3). Initial results from these measurements have been described in refs 19–23, presenting complete mean annual sums and mean seasonal cycles of NPP and autotrophic respiration (R_a). This methodology has shown close agreement with independent eddy covariance data on seasonal and annual timescales (Extended Data Fig. 1;

[1]Environmental Change Institute, School of Geography and the Environment, University of Oxford, Oxford OX1 3QY, UK. [2]Department of Physical Geography and Ecosystem Science, Lund University, Sölvegatan 12, 223 62 Lund, Sweden. [3]Universidad Nacional San Antonio Abad de Cusco, Apartado Postal Nro 921, Cusco, Perú. [4]Museo de Historia Natural Noel Kempff Mercado, Universidad Autónoma Gabriel Rene Moreno, Av. Irala 565, Casilla 2489, Santa Cruz, Bolivia. [5]Universidade Federal do Pará, Instituto de Geociências, Faculdade de Meteorologia, Rua Augusto Correa, n° 01, CEP 66075 - 110, Belém, Pará, Brazil. [6]IPAM Instituto de Pesquisa Ambiental da Amazônia Rua Horizontina, 104, Centro, 78640-000 Canarana, Mato Grosso, Brazil. [7]Department of Geography, College of Life and Environmental Sciences, University of Exeter, Exeter EX4 4RJ, UK. [8]School of Geosciences, University of Edinburgh, Edinburgh EH9 3FF, UK. [9]Research School of Biology, Australian National University, Canberra, Australian Capital Territory 2601, Australia. [10]School of Geography, University of Leeds, Leeds LS2 9JT, UK.

the slope is within the error of a one-to-one line, 3.0 ± 7.8% (95% confidence interval))[24]. Here we synthesize and further analyse these results to focus specifically on the basin-wide trends before, during and after the 2010 drought, constrained by concurrent measurements in a larger network measuring woody NPP and mortality[4] and inversion studies monitoring changes in atmospheric CO_2 concentrations[5]. Of the thirteen plots, six experienced drought in 2010 (Extended Data Fig. 2). Of these six, three can be considered lowland humid forest more typical of Amazonia (on the basis of species composition and maximum cumulative water deficit (MCWD); see Methods), and three are drier forests at the southern margins of the Amazon forests.

Throughout the two-year period of study, the seven non-drought plots showed steady NPP, R_a and total plant carbon expenditure (PCE, the sum of NPP and R_a, or the carbon expended by the autotrophic metabolism of the ecosystem; Fig. 1, green lines). Total NPP was invariant throughout the drought period at all of our plots (Fig. 1c). Among the six drought-affected plots, there were differences between those in the dry lowlands (Fig. 1, red lines; $n = 3$) and those in the more humid areas (Fig. 1, black lines; $n = 3$). PCE in the humid lowland plots was constant at the start of the drought, but then both PCE and R_a decreased significantly ($P < 0.05$ and $P < 0.01$, respectively; paired t-test, $n = 3$ plots) into early 2011 relative to the 2009 baseline. The humid plots recovered to the 2009 baseline within a few months after the drought, but decreases in R_a at the three dry lowland plots persisted for a year after the 2010 drought (Fig. 1b). This short-term decrease in R_a (dominated by changes in rhizosphere and stem respiration; Extended Data Fig. 7) is in contrast to the results from a multi-annual experimental drought in which R_a increased (dominated by changes in leaf respiration)[19].

PCE should roughly equal total photosynthesis in an ecosystem over annual to multi-annual timescales, with any discrepancy between the two on shorter (monthly) timescales being caused by changes in unmeasured carbon pools such as NSC reserves. A decrease in PCE must therefore equal an equivalent decrease in GPP during a previous period. At our humid drought sites, PCE decreased by 1.90 ± 1.04 Mg C ha^{-1} yr^{-1} (95% confidence interval) during and after the drought period compared with the 2009 baseline (yellow region of Fig. 1a). *In situ* measurements of light-saturated maximum photosynthesis made at a subset of our plots indicate that photosynthesis did decrease significantly ($P < 0.001$, t-test, $n = 20$ trees per plot) during the drought period in comparison with non-drought conditions on the same trees, indicating that the drought was the cause of the decrease in PCE (Extended Data Fig. 3). This measured decrease in photosynthesis is of a similar magnitude to modelled decreases in photosynthesis from drought in eastern Amazonia[25]. We speculate that the asynchrony between the decrease in PCE and the start of the drought indicates that the forests relied on NSC reserves to maintain constant growth and respiration initially during the drought period (Extended Data Fig. 4). Towards the middle of the drought period, R_a decreased in the rhizosphere and stems, whereas NPP and growth continued to remain relatively constant. Because autotrophic respiration consists of maintenance (non-growth) respiration and the respiratory costs associated with growth, this suggests that maintenance respiration not associated with growth must have declined. The decrease in R_a continued after the end of the drought period, potentially allowing the replenishment of the NSC stores once normal photosynthesis resumed (Extended Data Fig. 4). Drought decreased PCE by a larger amount in dry-zone plots than in humid-zone plots, with total PCE continuing to decline into 2011. The greater total decline in PCE is indicative of a larger percentage decrease in total photosynthesis during the drought at the drier plots, a plot-scale observation that matches our *in situ* leaf-level measurements (Extended Data Fig. 3). Our data show little change in net heterotrophic respiration in the humid drought plots (Fig. 1d, black line, and Extended Data Results), and this suggests that the drought forest plots were first a net C source in 2010 due to suppressed photosynthesis, and then a net C sink in early 2011 as photosynthesis returned to normal, while R_a in the stems and rhizosphere

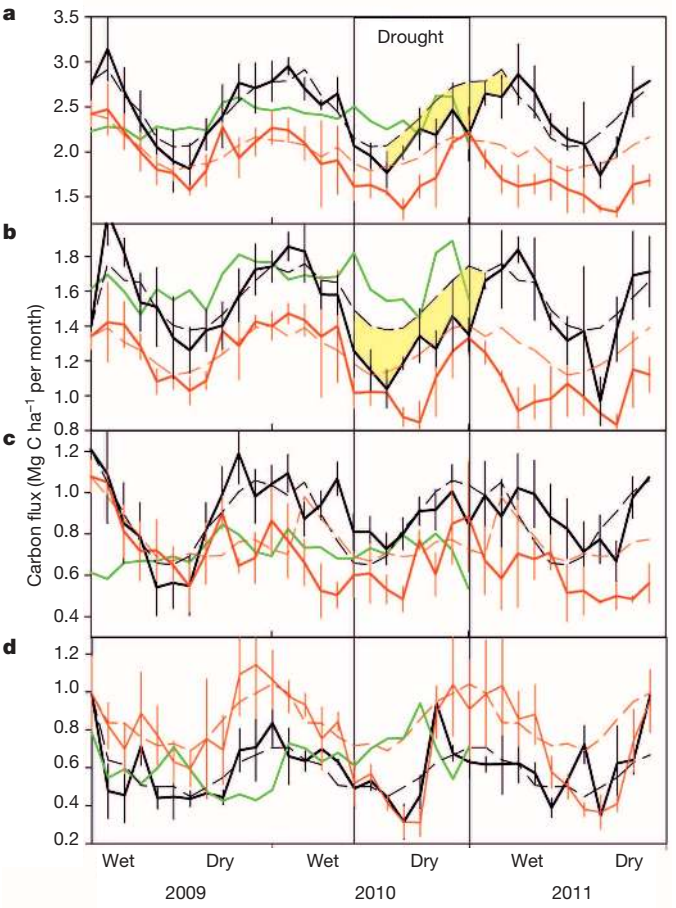

Figure 1 | Impact of drought on carbon fluxes. Results from the forests for the three drought-affected forest plots in humid lowland zones (solid black lines), the three drought-affected forest plots in dry lowland zones (solid red lines), and the seven non-drought plots (solid green lines). **a**, Total PCE; **b**, total R_a; **c**, total NPP; **d**, heterotrophic soil respiration. Error bars indicate the standard error of mean plot differences. For visual clarity we do not include all error bars. Dashed lines show 'normal' (2009; pre-drought) estimates smoothed with a span of 5 months during 2010 and 2011 for the lowland plots (black) and the dry lowland plots (red). The vertical area labelled 'drought' represents the approximate period of the drought. The areas highlighted in yellow represent the drought anomaly or the impact of the drought on total plant carbon expenditure (numerically equivalent to GPP) and R_a.

remained slightly suppressed in comparison with previous periods (Extended Data Figs 4 and 7).

There was strong seasonality in the components of NPP, with peaks in leaf growth generally anti-correlated with the peaks in woody growth. Hence variation in seasonal growth rates was driven more by shifts in the allocation of NPP than by variation in its total magnitude[26]. NPP allocation in the non-droughted plots did not change significantly between 2009 and 2010 (Fig. 2a–d, green lines). In the droughted plots there were no significant shifts in allocation patterns during the drought period itself, but in the 6 months after the drought there was a significant shift in C allocation for both the humid and dry lowland plots after the drought period away from fine-root growth ($P < 0.01$, paired t-test, $n = 3$) and towards canopy growth (a combination of leaf area index and litterfall (see Methods); $P < 0.05$, paired t-test, $n = 3$) (Fig. 2a–d, red and black lines). Droughts typically increase leaf fall, a strategy that is thought to minimize drought-induced xylem embolisms, and they can also cause temperature-related leaf damage as evaporative cooling decreases[8]. Preferential allocation of carbon towards the canopy in the year after the drought is therefore consistent with known physiological drought responses, and probably represents additional carbon

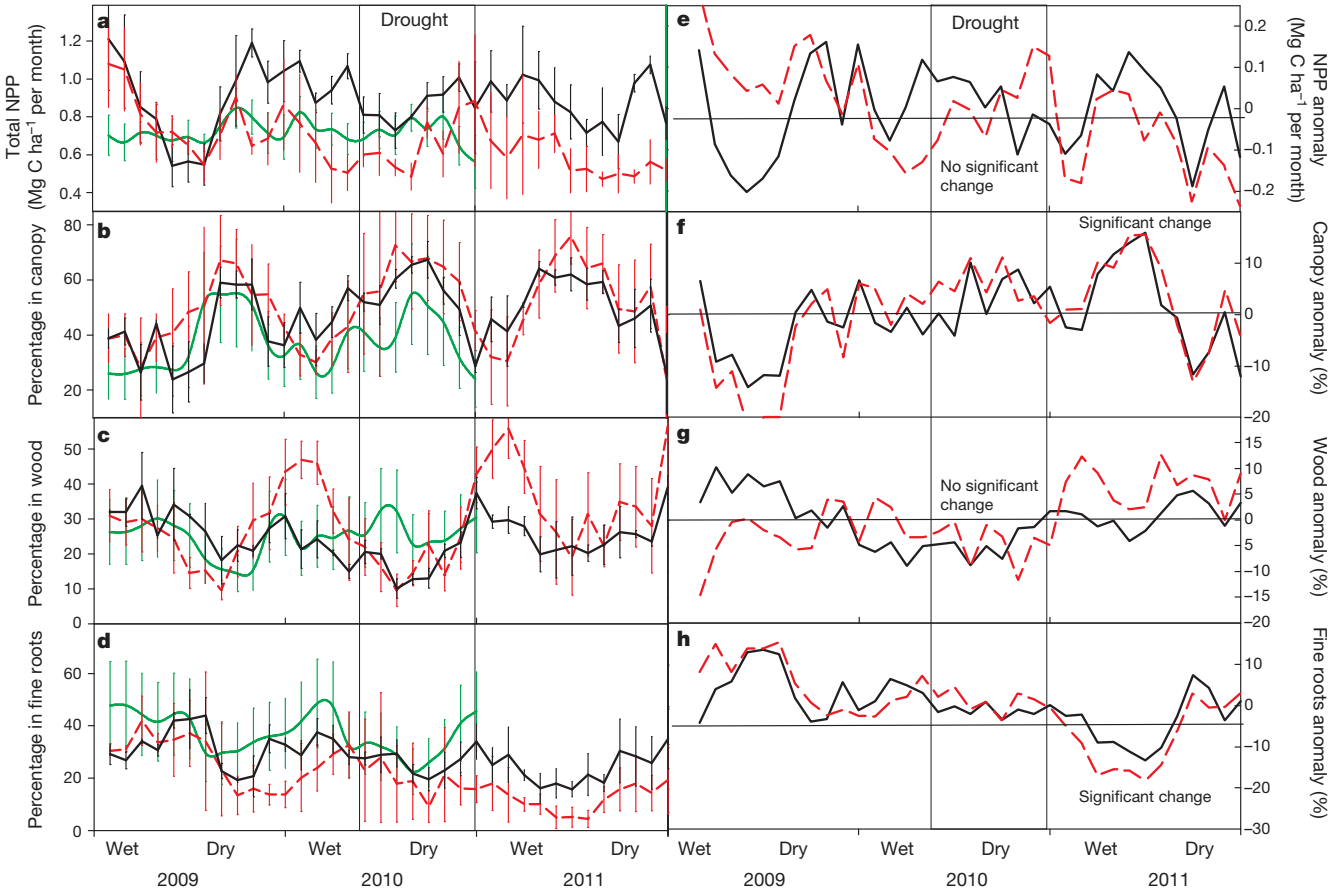

Figure 2 | Impact of drought on carbon allocation. **a**–**d**, Total NPP (**a**), mean carbon allocation to canopy (**b**), mean carbon allocation to wood (**c**) and mean carbon allocation to fine roots (**d**) for non-drought lowland plots (green solid lines; $n = 7$), drought plots in the humid lowlands (black solid lines; $n = 3$) and drought plots in the dry lowlands (red dashed lines; $n = 3$). **e**–**h**, Seasonally detrended anomaly data for each variable on the left. All error bars are standard errors across plots. The vertical bar labelled 'drought' represents the approximate period of the drought. Significant change was determined with a paired *t*-test comparing six-month periods during and after the drought with equivalent months in 2009 for all plots.

to replenish lost and damaged leaves and thereby rebuild photosynthetic capacity. The significant shift away from fine-root growth was surprising, because it has often been assumed that fine-root growth might increase during a drought, but the shift may simply be a reflection of the immediate priority of replacing lost canopy cover instead of a long-term shift away from root growth (for longer-term allocation patterns see Extended Data Fig. 5 and ref. 26).

Individual tree mortality rates roughly doubled at our droughted plots, showing a marginally significant increase ($P = 0.06$, paired one-tailed *t*-test, $n = 5$) from a long-term mean of 1.6 ± 0.6% (Tambopata; $n = 3$) and 2.0 ± 0.4% (Kenia; $n = 2$) to peaks of 3.6% (Tambopata) and 6.7% (Kenia) after the drought (Extended Data Fig. 6c). Mortality remained relatively stable at the non-droughted plots. We tested mortality in a bigger subset of plots at Tambopata and Caxiuanã going back ~30 years at some plots (Extended Data Results) and found that rates of biomass loss increased significantly ($P < 0.05$, Wilcoxon signed-rank test) at Tambopata (drought; $n = 9$) but not at Caxiuanã (no drought; $n = 6$). Committed carbon released as a result of mortality increased from a basin-wide average of 1.6% annual[27] to 3.9% in Tambopata and 2.3% in Kenia (Fig. 3e). Similar drought-induced mortality was also seen across the wider basin after the 2005 drought[4]. The Bolivian plots experienced more severe drought ($MCWD_{anom} < -240$ mm), and here more trees died more quickly than in the Peruvian plots, which were less strongly droughted ($MCWD_{anom} = -51$ mm). Our data indicate that mortality rates peaked 1–2 years after the drought, consistent with the hypothesis that trees were weakened during the drought from decreased maintenance but only succumbed later[19].

Plant carbon expenditure was significantly related ($P < 0.05$, linear regression) and autotrophic respiration was marginally significantly related ($P = 0.08$, linear regression) to the anomaly in MCWD for both annual sums ($n = 13$ individual plots for 2009 minus 2010; $PCE_{anom} = -1.0 + 0.011 \times MCWD_{anom}$, $r^2 = 0.34$, with a standard error on the slope of ±0.004; Fig. 3a, b). The anomaly in NPP, in contrast, showed no significant relationship with the MCWD anomaly (Fig. 3c; $P > 0.10$). We combine a TRMM (version 7; years 1998–2012)-based $MCWD_{anom}$ for each TRMM pixel in the Amazon in 2010 and 2011 with the slope of the above equation (with an intercept of zero) to estimate that mean net total photosynthesis decreased by 0.38 Pg C (0.23–0.53 Pg C) in 2010 compared with 2011, based on a mean South American tropical forested area of 6.77×10^6 km^2 (Fig. 3d). For the same period, an Amazonia-focused atmospheric inversion modelling study estimated a decreased flux of 0.25 ± 0.14 Pg C in 2010 relative to 2011 from decreased photosynthesis, which is within our error estimates[5].

Why would trees prioritize growth over maintenance or defence during and after a drought? This strategy makes sense when viewed from an eco-evolutionary standpoint, where any decrease in growth of an individual tree puts that tree at a competitive disadvantage by increased risk of loss of resources (light, water or nutrients) to neighbours[6]. We speculate that this decrease in maintenance and defence led to our plot-level increase in mortality. Thus, although such a drought-induced strategy may decrease the mean performance per tree in the forest through increased mortality, it is still likely to be selected for on an individual basis given the evolutionary constraints proposed by game theory[28]. In other words, this strategy increases mortality for a small proportion of

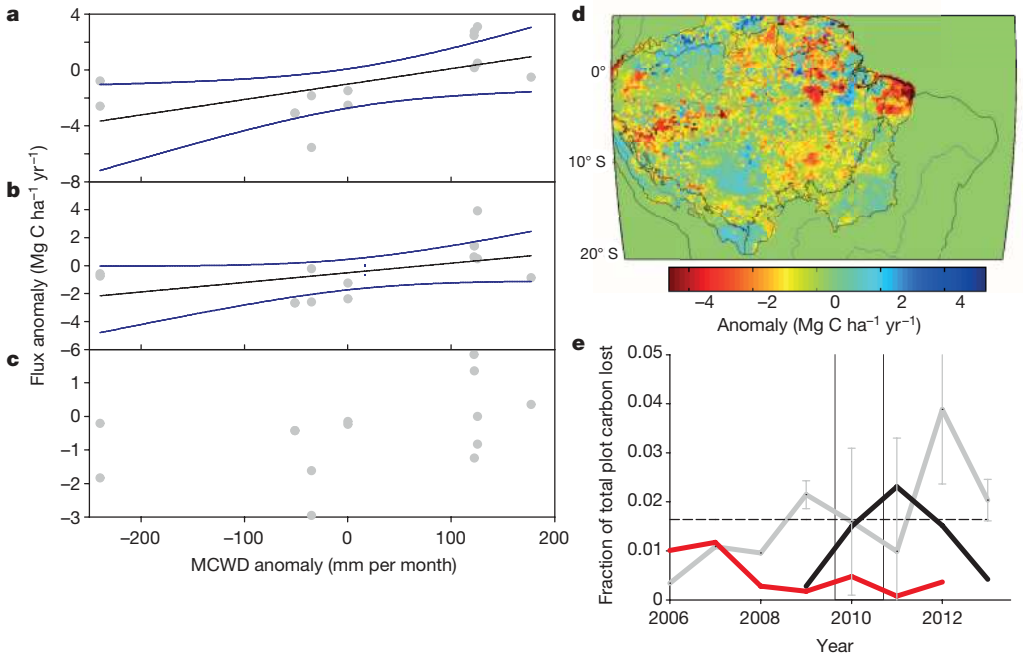

Figure 3 | Estimated impact of drought on the basin-wide flux of CO_2. **a–c**, Shifts in annual fluxes in 2010 relative to 2009 for each individual plot for plant carbon expenditure ($PCE_{anom} = -1.0 + 0.011 \times MCWD_{anom}$, equal to GPP_{anom} over longer timescales; $r^2 = 0.34$, $P < 0.05$) (**a**), R_a ($R_{a,anom} = -0.51 + 0.007 \times MCWD_{anom}$, $r^2 = 0.23$, $P < 0.1$) (**b**) and NPP (not significant) (**c**), plotted against the shift in MCWD in 2010 relative to 2009. **d**, Estimate of basin-wide anomaly in GPP (2011 minus 2010; assumed equal to PCE) based on the TRMM (version 7)-calculated CWD anomaly (mm per month) and the slope of the linear regression found in **a**. We contrast 2010 with 2011 to compare with the atmospheric inversion measurements collected during this period[5]. **e**, Mortality rates as fraction of plot biomass for Peruvian drought plots (grey line; $n = 3$; error bars are standard errors), Bolivian drought plots (black line; $n = 2$) and no-drought plots (red line; $n = 3$). Mean Amazonian background tree mortality (no drought) is shown as a thin black dashed line (from fig. 3 in ref. 27).

trees because most are locked in to growth competition with neighbours. Such unexpected carbon allocation patterns have been theorized previously, but before now they have lacked much empirical support. For instance, trees may grow excess leaves not to improve carbon uptake but to shade out competition[29], or they may over-allocate carbon to root growth in shallow soil systems in response to competition[6].

Overall, our plot data indicate that drought suppressed total CO_2 uptake with little reduction in growth; less carbon was therefore available to the trees for defence and maintenance. Decreased soluble carbon availability may have also increased tree mortality from embolisms and cavitation because NSCs (sugars) may be involved in sensing and reversing embolism[18]. The debate over drought-induced tree mortality is often framed as being caused by carbon starvation, water cavitation or biotic attack, but the three are often intertwined[30] because during drought there is less carbon available to fend off all three threats. This insight and new mechanistic understanding can help to improve predictions of the impact of future climate change on tropical forests.

Online Content Methods, along with any additional Extended Data display items and Source Data, are available in the online version of the paper; references unique to these sections appear only in the online paper.

Received 25 February; accepted 22 December 2014.

1. Lewis, S. L., Brando, P. M., Phillips, O. L., van der Heijden, G. M. F. & Nepstad, D. The 2010 Amazon drought. *Science* **331,** 554 (2011).
2. Gloor, M. *et al.* Intensification of the Amazon hydrological cycle over the last two decades. *Geophys. Res. Lett.* **40,** 1729–1733 (2013).
3. Solomon, S. *et al.* (eds) *Climate Change 2007: The Physical Science Basis* (Cambridge Univ. Press, 2007).
4. Phillips, O. L. *et al.* Drought sensitivity of the Amazon rainforest. *Science* **323,** 1344–1347 (2009).
5. Gatti, L. V. *et al.* Drought sensitivity of Amazonian carbon balance revealed by atmospheric measurements. *Nature* **506,** 76–80 (2014).
6. Franklin, O. *et al.* Modeling carbon allocation in trees: a search for principles. *Tree Physiol.* **32,** 648–666 (2012).
7. da Costa, A. C. L. *et al.* Effect of 7 yr of experimental drought on vegetation dynamics and biomass storage of an eastern Amazonian rainforest. *New Phytol.* **187,** 579–591 (2010).
8. Nepstad, D. C. *et al.* The effects of partial throughfall exclusion on canopy processes, aboveground production, and biogeochemistry of an Amazon forest. *J. Geophys. Res.* **107** (D20), 8085 (2002).
9. Xu, L. A. *et al.* Widespread decline in greenness of Amazonian vegetation due to the 2010 drought. *Geophys. Res. Lett.* **38,** L07402 (2011).
10. Saatchi, S. *et al.* Persistent effects of a severe drought on Amazonian forest canopy. *Proc. Natl Acad. Sci. USA* **110,** 565–570 (2013).
11. Saleska, S. R., Didan, K., Huete, A. R. & da Rocha, H. R. Amazon forests green-up during 2005 drought. *Science* **318,** 612 (2007).
12. Phillips, O. L. *et al.* Changes in the carbon balance of tropical forests: evidence from long-term plots. *Science* **282,** 439–442 (1998).
13. Meir, P., Metcalfe, D. B., Costa, A. C. L. & Fisher, R. A. The fate of assimilated carbon during drought: impacts on respiration in Amazon rainforests. *Phil. Trans. R. Soc. B* **363,** 1849–1855 (2008).
14. Townsend, A. R., Asner, G. P., White, J. W. C. & Tans, P. P. Land use effects on atmospheric C-13 imply a sizable terrestrial CO_2 sink in tropical latitudes. *Geophys. Res. Lett.* **29,** 1426 (2002).
15. Malhi, Y., Doughty, C. & Galbraith, D. The allocation of ecosystem net primary productivity in tropical forests. *Phil. Trans. R. Soc. B* **366,** 3225–3245 (2011).
16. Wurth, M. K. R., Pelaez-Riedl, S., Wright, S. J. & Korner, C. Non-structural carbohydrate pools in a tropical forest. *Oecologia* **143,** 11–24 (2005).
17. Dietze, M. C. *et al.* Nonstructural carbon in woody plants. *Annu. Rev. Plant Biol.* **65,** 667–687 (2014).
18. Sala, A., Woodruff, D. R. & Meinzer, F. C. Carbon dynamics in trees: feast or famine? *Tree Physiol.* **32,** 764–775 (2012).
19. da Costa, A. C. L. *et al.* Ecosystem respiration and net primary productivity after 8–10 years of experimental through-fall reduction in an eastern Amazon forest. *Plant Ecol. Divers.* **7,** 7–24 (2014).
20. Araujo-Murakami, A. *et al.* The productivity, allocation and cycling of carbon in forests at the dry margin of the Amazon forest in Bolivia. *Plant Ecol. Divers.* **7,** 55–69 (2014).
21. Doughty, C. E. *et al.* The production, allocation and cycling of carbon in a forest on fertile terra preta soil in eastern Amazonia compared with a forest on adjacent infertile soil. *Plant Ecol. Divers.* **7,** 41–53 (2014).
22. Malhi, Y. *et al.* The productivity, metabolism and carbon cycle of two lowland tropical forest plots in south-western Amazonia, Peru. *Plant Ecol. Divers.* **7,** 85–105 (2014).
23. Rocha, W. *et al.* Ecosystem productivity and carbon cycling in intact and annually burnt forest at the dry southern limit of the Amazon rainforest (Mato Grosso, Brazil). *Plant Ecol. Divers.* **7,** 25–40 (2014).

24. Fenn, K., Malhi, Y., Morecroft, M., Lloyd, C. & Thomas, M. The carbon cycle of a maritime ancient temperate broadleaved woodland at seasonal and annual scales. *Ecosystems* http://dx.doi.org/10.1007/s10021-014-9793-1 (13 December 2014).
25. Fisher, R. A. *et al.* The response of an Eastern Amazonian rain forest to drought stress: results and modelling analyses from a throughfall exclusion experiment. *Glob. Change Biol.* **13,** 2361–2378 (2007).
26. Doughty, C. E. *et al.* Allocation trade-offs dominate the response of tropical forest growth to seasonal and interannual drought. *Ecology* **95,** 2192–2201 (2014).
27. Lewis, S. L. *et al.* Concerted changes in tropical forest structure and dynamics: evidence from 50 South American long-term plots. *Phil. Trans. R. Soc. B* **359,** 421–436 (2004).
28. King, D. A. A model analysis of the influence of root and foliage allocation on forest production and competition between trees. *Tree Physiol.* **12,** 119–135 (1993).
29. Hikosaka, K. & Anten, N. P. R. An evolutionary game of leaf dynamics and its consequences for canopy structure. *Funct. Ecol.* **26,** 1024–1032 (2012).
30. McDowell, N. G. *et al.* The interdependence of mechanisms underlying climate-driven vegetation mortality. *Trends Ecol. Evol.* **26,** 523–532 (2011).

Supplementary Information is available in the online version of the paper.

Acknowledgements We thank P. Brando and Tanguro partners for logistical support and advice. This work is a product of the Global Ecosystems Monitoring (GEM) network (http://gem.tropicalforests.ox.ac.uk) and the RAINFOR and ABERG research consortia, and was funded by grants to Y.M. and O.L.P. from the Gordon and Betty Moore Foundation to the Amazon Forest Inventory Network (RAINFOR) and the Andes Biodiversity and Ecosystems Research Group (ABERG), and grants from the UK Natural Environment Research Council (NE/D01025X/1, NE/D014174/1, NE/F002149/1 and NE/J011002/1), the NERC AMAZONICA consortium grant (NE/F005776/1) and the EU FP7 Amazalert (282664) GEOCARBON (283080) projects. Some data in this publication were provided by the Tropical Ecology Assessment and Monitoring (TEAM) Network, a collaboration between Conservation International, the Missouri Botanical Garden, the Smithsonian Institution and the Wildlife Conservation Society, and partly funded by these institutions, the Gordon and Betty Moore Foundation, and other donors. T.R.F. is supported by a National Council for Scientific and Technological Development (CNPq, Brazil) award. P.M. is supported by an ARC fellowship award FT110100457; O.L.P. is supported by an ERC Advanced Investigator Award and a Royal Society Wolfson Research Merit Award; Y.M. is supported by an ERC Advanced Investigator Award and by the Jackson Foundation. C.E.D. acknowledges funding from the John Fell Fund.

Author Contributions C.E.D., Y.M. and D.B.M. designed and implemented the study. Y.M. conceived the GEM network, C.E.D., D.B.M., C.A.J.G. and Y.M. implemented it, and O.L.P. contributed to its development. C.E.D. analysed the data. C.E.D., C.A.J.G., F.F.A., D.G., W.H.H., J.E.S., A.A., M.C.C., A.C.L.C., T.F., A.M., W.R. and O.L.P. collected the data. C.E.D. wrote the paper with contributions from Y.M., O.L.P., P.M. and D.B.M.

Author Information Reprints and permissions information is available at www.nature.com/reprints. The authors declare no competing financial interests. Readers are welcome to comment on the online version of the paper. Correspondence and requests for materials should be addressed to C.E.D. (chris.doughty@ouce.ox.ac.uk).

METHODS

We measured total NPP and autotrophic respiration at thirteen 1-ha plots (plots described individually below) throughout the Amazon basin in the period 2009–2010 (and 2009–2011 or 2009–2012 for droughted plots). A detailed description of each measurement is listed in Extended Data Tables 1–3. Total measured NPP included canopy, woody, and fine-root NPP. In our seasonal estimates of NPP we exclude several smaller components such as branch fall (although branch-fall data are shown in Extended Data Fig. 6), herbivory, coarse root and small-tree (<10 cm) NPP that we have included in previous estimates of these sites. We calculate leaf flush by calculating the change in leaf area index, LAI ($m^2\,m^{-2}$), multiplied by the mean specific leaf area ($m^2\,g^{-1}$), and adding this to leaf litterfall by following a procedure from ref. 31. Total estimated autotrophic respiration consisted of rhizosphere respiration (that is, respiration from roots, mycorrhizae and exudate-dependent soil microbes), woody respiration and canopy respiration. Each component was measured every 1–3 months, except for canopy respiration, which was measured only 1–2 times per plot at the leaf level but scaled to the canopy scale using monthly LAI partitioned into sun and shade components. Seasonal changes in autotrophic respiration during and following drought are due to monthly measured rhizosphere and woody tissue (stem) respiration, not canopy (leaf) respiration (Extended Data Fig. 7). Detailed information on the methodology and graphs showing data from each individual component are also available from a series of companion papers[19–23,32,33]. Each of these site papers includes a full spatial and scaling error analysis for each measurement, so, for brevity, we do not include them here. All raw data inputs are available on request from the authors or from http://gem.tropicalforests.ox.ac.uk/.

Photosynthesis. Light-saturated leaf photosynthesis was measured at two plots in Bolivia in the peak of the drought (November 2010) and during a non-drought period (June 2011) on the same ~20 individual trees (12 different species from plot A and 17 species from plot B) in the plot, using canopy-top cut branches (immediately recut under water to restore hydraulic conductivity). These measurements are compared with leaf photosynthesis measurements in the Tapajos, Brazil, on attached (not cut) canopy top leaves accessed via three walk-up towers, to test whether A_{sat} (light-saturated photosynthesis) would be expected to decrease during a typical (non-severe) dry season, and the measurements were taken at the start of a typical dry season to the end of the dry season (Extended Data Fig. 3; methodological details in Extended Data Tables 1–3).

Climate. We classified our drought sites according to anomalies in cumulative water deficit (CWD) based on precipitation data collected from automatic weather stations at each of the plots (Skye Instruments). Six of our 13 plots experienced drought in 2010 (negative CWD anomalies for more than half the year), with a mean CWD anomaly of −107 mm in October and a mean maximum CWD (MCWD) of −135 mm, meaning that the driest month on average had a water deficit 135 mm greater than in a normal year (Extended Data Fig. 2). This varied regionally: the highest MCWD was in the Bolivian sites ($MCWD_{anom} = -240$ mm) and the lowest was in the lowland Peruvian sites ($MCWD_{anom} = -51$ mm). We used Tropical Rainfall Monitoring Mission (TRMM) data from January 1998 to December 2012 (TRMM version 7) to calculate for each pixel the maximum monthly CWD anomaly (Extended Data Fig. 2). The basin-wide median $MCWD_{anom}$ for 2010 for droughted tropical forest regions was 136 mm (excluding $MCWD_{anom} \geq 0$ mm). This implies that the mean of our droughted plots had a moisture anomaly equivalent to the basin-wide 'typical' Amazon drought for 2010 (Extended Data Fig. 2), but also that our plots did not experience the more severe drought seen by some regions of Amazonia.

Statistics. All data were tested for normality, and if they were normal we did a two-tailed paired *t*-test using Sigmaplot (Systat Software Inc.). If normality was not passed, as with the mortality data, we used a Wilcoxon signed-rank test. We used a two-tailed test except for mortality, for which we expected the change to be in one direction and therefore used a one-tailed test. We calculated 95% confidence intervals by multiplying the standard error by 1.96.

Additional mortality data. For the additional RAINFOR analyses for Tambopata and Caxiuanã, interval-by-interval loss rates in each plot were computed by following standard RAINFOR field and ForestPlots.net data protocols (see, for example, refs 34, 35). At Caxiuanã, data were collected by the TEAM network, whose protocols are closely based on RAINFOR models. These include multiple repeated diameter measurements of the same tree at 1.3 m or above buttresses (allowing where necessary for changes in point of measurement), high-resolution botanical identifications of hundreds of tree species at each site, and the use of taxon-specific wood density values, to derive from each individual tree at least 10 cm in diameter the stand-level values of biomass and biomass dynamics. We used a generalized region-specific height–diameter biomass allometry[36]. Because here the question is simply whether the 2010 drought coincided with mortality changes in each site, and not what the precise values of mortality were for individual intervals and plots, we did not attempt to account for the small effects of slightly varying census-interval lengths on wood production rates. Data were downloaded from ForestPlots.net in October 2014 and from the TEAM database in April 2013.

Site descriptions of thirteen 1-ha plots. Plots with drought in 2010. The Kenia plots ($n = 2$, 1-ha plots) were established and monitored on private property at the Hacienda Kenia in Guarayos Province, Santa Cruz, Bolivia (16.0158° S, 62.7301° W) from January 2009. The plots are 2 km apart and are situated on inceptisols with relatively high fertility (high cation exchange capacity and phosphorus concentration) and low acidity compared with eastern Amazonian forests. The plots experienced almost identical climate and had sandy loam soil with 76% sand content. However, one plot was located on a shallow soil (<1 m depth) over pre-Cambrian bedrock, leading to lower available water (we term this plot Kenia-B). The second plot was located on deeper soils in a slight topographic depression (henceforth termed Kenia-A). These differences in drainage and soil depth had an effect on forest composition at this ecotone, with Kenia-A hosting a more humid forest type typical of Amazonian forests and Kenia-B a drier forest type typical of *chiquitano* dry forests. For further details see ref. 20.

The Tanguro plots ($n = 2$, 1-ha plots) are located on the Fazenda Tanguro (~80,000 ha) in Mato Grosso state, about 30 km north of the southern boundary of the Amazon rainforest in Brazil (13.0765° S, 52.3858° W). The soil type at the site is a red–yellow alic dystrophic latosol (RADAM Brazil, 1974; Brazilian soil classification), a relatively infertile sandy ferralsol (FAO classification) or oxisol (Haplustox; US Department of Agriculture classification scheme), the groundwater is at ~15 m depth, and no layers of soil prevent root penetration through the soil profile. These soils are among the least fertile in Amazonia and are widespread across eastern Amazonia. The vegetation is closed-canopy, old-growth forest with a relatively low mean canopy height (20 m) and relatively low plant species diversity (97 species of trees and lianas greater than 10 cm DBH (diameter at 1.3 m stem height above the ground)) when compared with the wetter forests typical of the central Amazon. For further details see ref. 23.

The Tambopata study plots ($n = 2$, 1-ha plots) are located in the Tambopata reserve (TAM-05, 12.837° S, 69.2937° W; TAM-06, 12.828° S, 69.2690° W), in the Madre de Dios region of Peru. The geomorphology of the study region is based on old floodplains of the meandering Tambopata River. TAM-05 is situated on a Pleistocene terrace (<100 kyr old). The soil at TAM-05 is a haplic cambisol (WRB taxonomy), and that at TAM-06 is a haplic alisol[37]. We incorporate mortality data from an additional nearby plot (TAM-09). No hardpan layers of soil prevent root penetration through the soil profile. For further details see ref. 22.

We divided these six plots into three lowland plots (TAM-05, TAM-06 and Kenia-A; black lines in Figs 1 and 2) and three dry-lowland plots (the two Tanguro plots and Kenia-B; red lines in Figs 1 and 2). Distinction of dry-lowland plots was made by using mean MCWD for Tanguro and by species composition for Kenia-B with drier forest type species typical of *chiquitano* dry forests.

Plots with no drought in 2010. The San Pedro site ($n = 2$, 1-ha plots) at 13.0491° S, 71.5365° W is located in the Kosñipata Valley, in the cultural buffer zone of the Parque Nacional del Manú, Cusco, Peru. The two plots at San Pedro lie very close to the transition between upper and pre-montane forest zones, which occurs in this valley at ~1,500–2,000 m. Although data on cloud cover frequency and cloud base elevation in the plots over the annual cycle are difficult to obtain, SP 1750 is immersed for longer periods than SP 1500 during the austral winter months. SP 1500 is estimated to be near the lower limit of the cloud base. For further details see ref. 33.

The Wayqecha and Esperanza plots ($n = 2$, 1-ha plots) (Wayqecha, RAINFOR plot code WAY-01, 13.1751° S 71.5948° W; Esperanza, RAINFOR plot code ESP-01) plots are high-elevation cloud forest located in the cultural buffer zone of the Parque Nacional del Manú, Cusco, Peru at ~3,000 m elevation. The two plots lay a few hundred metres below the treeline transition to high-elevation grasslands. For further details see ref. 32.

The Caxiuanã plots (CAX-08 and CAX-06; $n = 2$, 1-ha plots) are located in Caxiuanã National Forest Reserve, Pará, in the eastern Brazilian Amazon. The *terra preta* plot (1.8560° S, 51.4352° W; plot code CAX-08 in the RAINFOR Amazon forest inventory network) was a late successional forest with a large proportion of fruit trees, on an isolated patch (<2 ha) of fertile dark earth or *terra preta do Indio*. The original ferralsol soils became progressively enriched by the activities of local inhabitants between AD 1280 and 1600 (ref. 38). The species composition of the *terra preta* plot was that of an old abandoned agroforestry system, with Brazil nut (*Bertholletia excelsa*) and kapok (*Ceiba pentandra*) as well as palaeotropical tree crops including coffee (*Coffea*) and orange (*Citrus*). The water-side location of the *terra preta* plot results in a substantially different microclimate from that of the inland tower plot, with high solar radiation (the large cool water area of the bay suppresses cloud formation close to the bay) and higher temperatures. The 'tower' plot (CAX-06; 1.7198° S, 51.4581° W) was a tall primary forest (35 m canopy height) situated on a clay-rich geric alumnic ferralsol (alumnic, hyperdistric, clayic) near an

eddy covariance flux tower, with species composition typical of eastern Amazonia. For further details see ref. 21.

The Caxiuanã plot (TFE-control; $n = 1$, 1-ha plot) is the control plot of an experimental drought study which is ~2 km south of the tower plot mentioned above (1.7279° S, 51.4680° W). It is a largely undisturbed *terra firme* forest, of the type widespread across eastern Amazonia. The study plot is located on highly weathered vetic acrisols typical of upland forests in the eastern Amazon, with a thick stony laterite layer at 3–4 m depth. The site elevation is 15 m above river level in the dry season, and the water table has occasionally been observed at a soil depth of 10 m during the wet season. For further details see ref. 19.

Extended Data results. Heterotrophic respiration. Soil heterotrophic respiration showed no significant change during the drought period in the droughted humid lowland plots (Fig. 1d, black line; $n = 3$) and no significant change with CWD anomaly ($P > 0.05$). There was a slight suppression of heterotrophic soil respiration near the start of the drought, but this was compensated for by a larger than normal increase in heterotrophic soil respiration later in the drought as some rains (although much lower than normal) arrived (Fig. 1d, black line). However, in contrast, the droughted dry lowland plots did show a large decrease in soil heterotrophic respiration at the start of the drought in comparison with 2009 (although only marginally significant: $P < 0.1$, $n = 3$) (Fig. 1d, red line), but these regions are a geographically small part of the basin and their overall influence on basin wide fluxes is likely to be small. Mean temperatures were similar in 2010 and 2011 and therefore any change in heterotrophic flux was most likely to have been driven by moisture (Extended Data Fig. 2). Deadwood respiration was initially suppressed during the dry season of the drought year, but this was compensated for by a large gain once the rains started, leading to no net annual change in deadwood respiration from the drought (Extended Data Fig. 6). Branch fall did not increase during the drought and, in fact, slightly decreased, possibly because of lower wind speeds from decreased storm activity (Extended Data Fig. 6). Our data show little net change in heterotrophic respiration; we therefore estimate that the drought forest plots were first a net C source in 2010 as a result of suppressed photosynthesis, and then a net C sink in early 2011 as photosynthesis returned to normal but R_a remained slightly supressed compared with previous periods, an observation in line with a recent atmospheric inversion study of the Amazon basin[5].

Shifts in carbon allocation. In two of the plots (Kenia-A and Kenia-B), NPP allocation shifted towards roots in the second year after the drought, possibly to alleviate water stress for future droughts, or to increase nutrient uptake to track recovered carbon uptake (Extended Data Fig. 5; NPP allocation patterns at this site are explored in detail in ref. 26). However, allocation responses to drought vary strongly by site. For instance, in two lowland Peruvian plots that experienced milder drought, NPP instead shifted back towards woody growth in the second year after the drought (Extended Data Fig. 5), whereas in two dry lowland Brazilian plots that experienced moderate drought, woody growth increased in the year after the drought at the expense of canopy and fine-root growth (Extended Data Fig. 5). The two plots hardest hit by the drought ($MCWD_{anom} = -240$ mm) showed a long-term decrease in allocation of NPP towards wood even though total NPP remained constant (Extended Data Fig. 5). This indicates that care should be taken in the interpretation of tree growth and dendrochronology results as proxies for productivity after drought, because they may be influenced more by shifting carbon allocation than by changes in total NPP. Our plots showed no significant change in woody NPP growth rates during the drought, although there was a small decline (Fig. 2g). Woody growth rates may actually have declined, but our sample size of three was too small to capture the signal statistically.

Additional mortality results. To see whether mortality increased more broadly in the regions surrounding our plots, we compared plots in the RAINFOR database near Tambopata (with drought according to our meteorological station data) with Caxiuanã (without drought in 2010). In Caxiuanã, we compared plots 1–6 (TEC-01 to TEC-06, using the RAINFOR code) for pre-2010 mortality (starting in 2003) with mortality from a census in late 2010. In Tambopata, we compared plots TAM-01 to TAM-08 for pre-2010 mortality (mostly starting in 1983) with mortality from a census in mid-2011. For this data set, we used a non-parametric Wilcoxon signed-rank test and found significant increase in biomass mortality following the 2010 drought in the larger Tambopata data set ($n = 9$, $P = 0.018$). This is in contrast with Caxiuanã (a no-drought site), where we also had high-resolution meteorological station data, and found no significant change after 2009 ($n = 6$, $P > 0.05$).

31. Doughty, C. E. & Goulden, M. L. Seasonal patterns of tropical forest leaf area index and CO_2 exchange. *J. Geophys. Res.* **113,** G00b06 (2008).
32. Girardin, C. A. J. *et al.* Productivity and carbon allocation in a tropical montane cloud forest in the Peruvian Andes. *Plant Ecol. Divers.* **7,** 107–123 (2014).
33. Huasco, W. H. *et al.* Seasonal production, allocation and cycling of carbon in two mid-elevation tropical montane forest plots in the Peruvian Andes. *Plant Ecol. Divers.* **7,** 125–142 (2014).
34. Quesada, C. A. *et al.* Basin-wide variations in Amazon forest structure and function are mediated by both soils and climate. *Biogeosciences* **9,** 2203–2246 (2012).
35. Lopez-Gonzalez, G., Lewis, S. L., Burkitt, M. & Phillips, O. L. ForestPlots.net: a web application and research tool to manage and analyse tropical forest plot data. *J. Veg. Sci.* **22,** 610–613 (2011).
36. Feldpausch, T. R. *et al.* Tree height integrated into pantropical forest biomass estimates. *Biogeosciences* **9,** 3381–3403 (2012).
37. Quesada, C. A. *et al.* Soils of Amazonia with particular reference to the RAINFOR sites. *Biogeosciences* **8,** 1415–1440 (2011).
38. Lehmann, J., Kern, D. C., Glaser, B. & Woods, W. I. *Amazonian Dark Earths: Origin, Properties, Management* (Kluwer Academic, 2003).
39. Malhi, Y. *et al.* The linkages between photosynthesis, productivity, growth and biomass in lowland Amazonian forests. *Global Change Biol.* http://dx.doi.org/10.1111/gcb.12859 (10 January 2015).
40. Malhi, Y. *et al.* Exploring the likelihood and mechanism of a climate-change-induced dieback of the Amazon rainforest. *Proc. Natl Acad. Sci. USA* **106,** 20610–20615 (2009).
41. Doughty, C. E. An *in situ* leaf and branch warming experiment in the Amazon. *Biotropica* **43,** 658–665 (2011).
42. da Rocha, H. R. *et al.* Seasonality of water and heat fluxes over a tropical forest in eastern Amazonia. *Ecol. Appl.* **14,** S22–S32 (2004).
43. Brando, P. M. *et al.* Abrupt increases in Amazonian tree mortality due to drought–fire interactions. *Proc. Natl Acad. Sci. USA* **111,** 6347–6352 (2014).
44. Chave, J. *et al.* Tree allometry and improved estimation of carbon stocks and balance in tropical forests. *Oecologia* **145,** 87–99 (2005).
45. Martin, A. R. & Thomas, S. C. A reassessment of carbon content in tropical trees. *PLoS ONE* **6,** e23533 (2011).
46. Metcalfe, D. B. *et al.* Factors controlling spatio-temporal variation in carbon dioxide efflux from surface litter, roots, and soil organic matter at four rain forest sites in the eastern Amazon. *J. Geophys. Res.* **112,** G04001 (2007).
47. Malhi, Y. *et al.* Comprehensive assessment of carbon productivity, allocation and storage in three Amazonian forests. *Global Change Biol.* **15,** 1255–1274 (2009).
48. Chambers, J. Q. *et al.* Respiration from a tropical forest ecosystem: Partitioning of sources and low carbon use efficiency. *Ecol. Appl.* **14,** S72–S88 (2004).

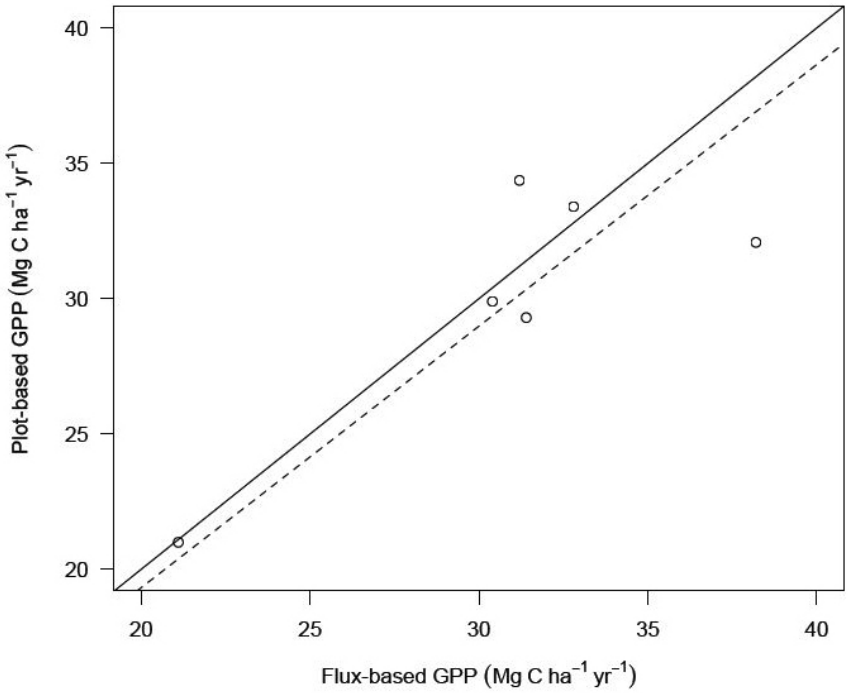

Extended Data Figure 1 | Comparison of plot-based and flux-based estimates of gross primary productivity (GPP) at six different sites worldwide. The black line represents 1:1; the dashed line represents a linear fit with a *y* intercept of 0. Slope = 0.97 ± 0.04, coefficient of determination = 0.61. If the Caxiuanã tower site is removed, then slope = 1.01 ± 0.03 and coefficient of determination = 0.87. Data points are from Manaus, Tapajos, Caxiuanã (Brazil), Wytham Woods (UK) and Lambir Hills (Malaysia). For further details see ref. 39.

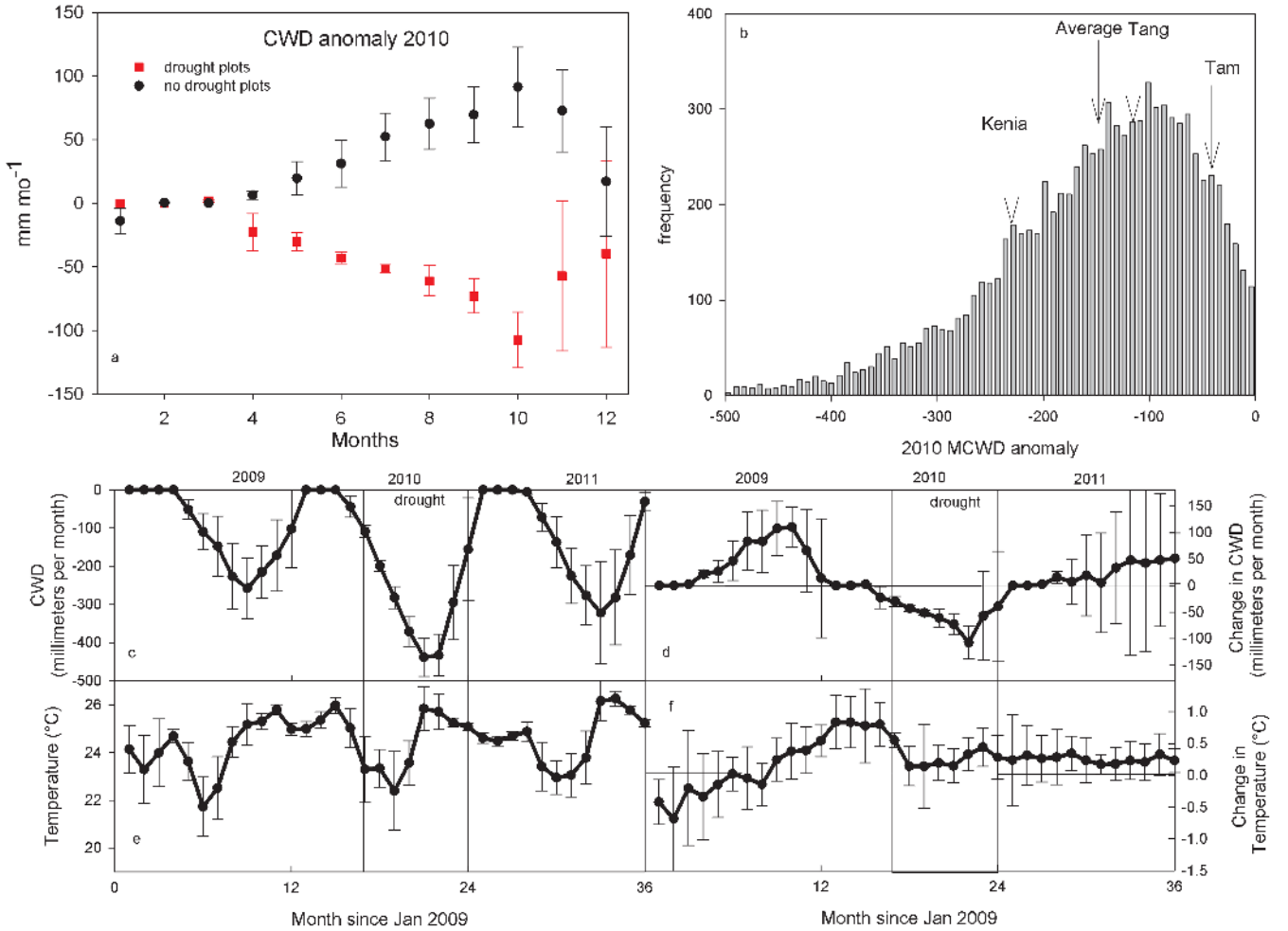

Extended Data Figure 2 | Climate data for the plots. **a**, Cumulative water deficit (CWD) anomaly for six droughted plots (red) and the remaining seven non-droughted plots (black) in 2010, on the basis of data from Skye instruments meteorological stations near each plot. Meteorology stations were set up in either ~2005 ($n = 4$) or ~2009 ($n = 4$). **b**, MCWD anomaly for 2010 (the minimum of CWD_{mean} minus CWD_{2010}) for the entire Amazon basin based on TRMM version 7 data (1998–2012). For clarity we do not show MCWD for non-droughted sites for which $MCWD_{anom} = 0$; this is the maximum potential value because by definition the wettest average month has a CWD value of 0). The arrows depict the site-specific MCWD anomaly for each drought area and average for all drought plots. **c**, **e**, Data from Skye instruments meteorological stations from January 2009 to December 2011 near our drought plots for cumulative water deficit (mm per month) (**c**) and air temperature (°C) (**e**). **d**, **f**, Anomalies for the same variables (mean values are average of all data from ~2005, ~2009–2011 or ~2009–2012). The drought period in our drought sites had a slightly lower average temperature during the drought than during the equivalent months of 2009 (24.6 °C versus 24.7 °C). The bar highlights the approximate period of the 2010 drought in the region based on CWD anomaly. To calculate CWD see ref. 40. Error bars are standard error differences between plots.

Plot	November 2010 (drought)	June 2011 (no drought)	Change
Kenia-A	2.92 ± 0.85	6.0 ± 0.98*	3.08 μmol m^{-2} s^{-1}
Kenia-B	−0.29 ±0.09	3.1 ± 0.67***	3.39 μmol m^{-2} s^{-1}

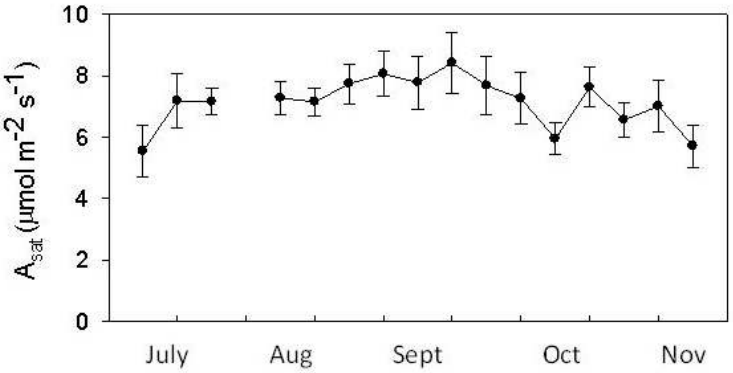

Extended Data Figure 3 | Leaf-level light-saturated photosynthesis measurements. Top: light-saturated (1,000 μmol m^{-2} s^{-1} irradiance, 25 °C, ambient CO_2) leaf gas exchange (μmol m^{-2} s^{-1}) (means ± s.e.m.) for a drought period (November 2010) and a non-drought period (June 2011) for sunlit branches (cut and rehydrated) on the same ~20 trees each season distributed evenly through the two (Kenia-A and Kenia-B) 1-ha plots. Asterisks indicate significant differences between the plots: *$P < 0.05$; ***$P < 0.001$. Bottom: weekly averaged leaf-level photosynthesis for eight species from three canopy walk-up towers measured at 1,000 μmol m^{-2} s^{-1} light and 30 °C between July (the start of the dry season) and November from the Tapajós, Brazil (see ref. 41 for further details and methodology). In the Tapajós the average dry season lasts from about July to about November. Note the lack of a decrease in photosynthesis during the dry season. Over this period, soil moisture decreases from ~0.45 to 0.40 m^3 m^{-3}, most of the decrease that occurs during the dry season[42]. These data suggest that a large (that is, 50%) sharp decline in leaf-level photosynthesis is not typical during an average dry season and that the declines shown in the table above are probably due to the 2010 drought.

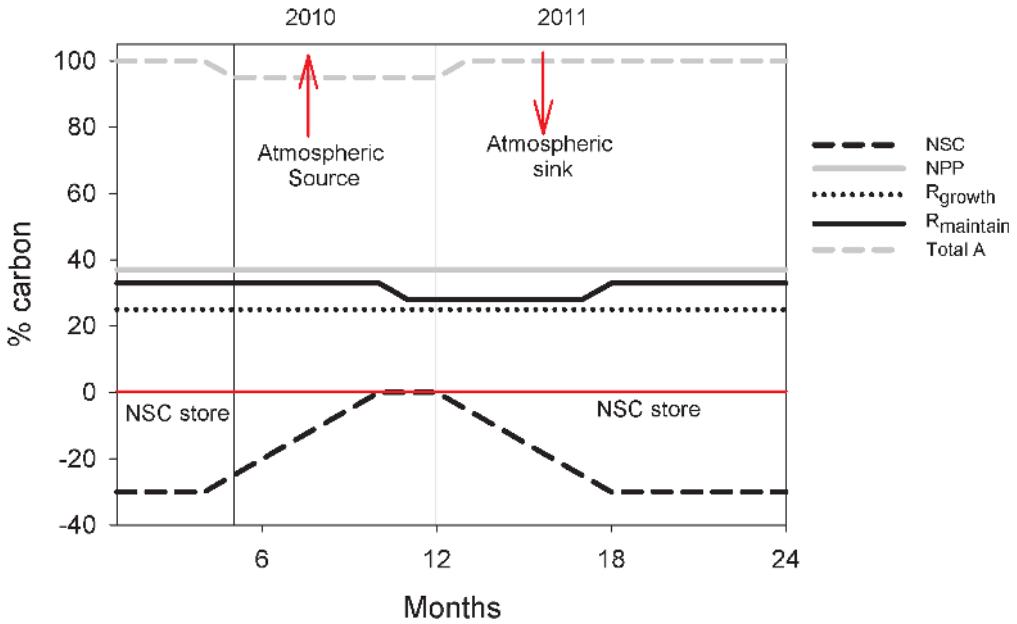

Extended Data Figure 4 | A conceptual model with simulated data of the impact of drought on the study sites. Total photosynthesis (grey dashed line; 100% represents average photosynthesis) decreased during the drought period (vertical bar). Total NPP (grey line, shown as a percentage of total photosynthesis) and growth respiration (R_{growth}) (black dotted line) remained constant, whereas maintenance respiration ($R_{maintain}$) (black line) decreased after NSC stores were depleted. Total NSC stores decreased (we define a negative value as NSC storage) during the drought period (the red line indicates a NSC storage of 0) and then increased at the end of the drought. Red arrows represent the timing of when the basin was a source (up) or a sink (down) of CO_2 to the atmosphere based on atmospheric inversion measurements from ref. 5.

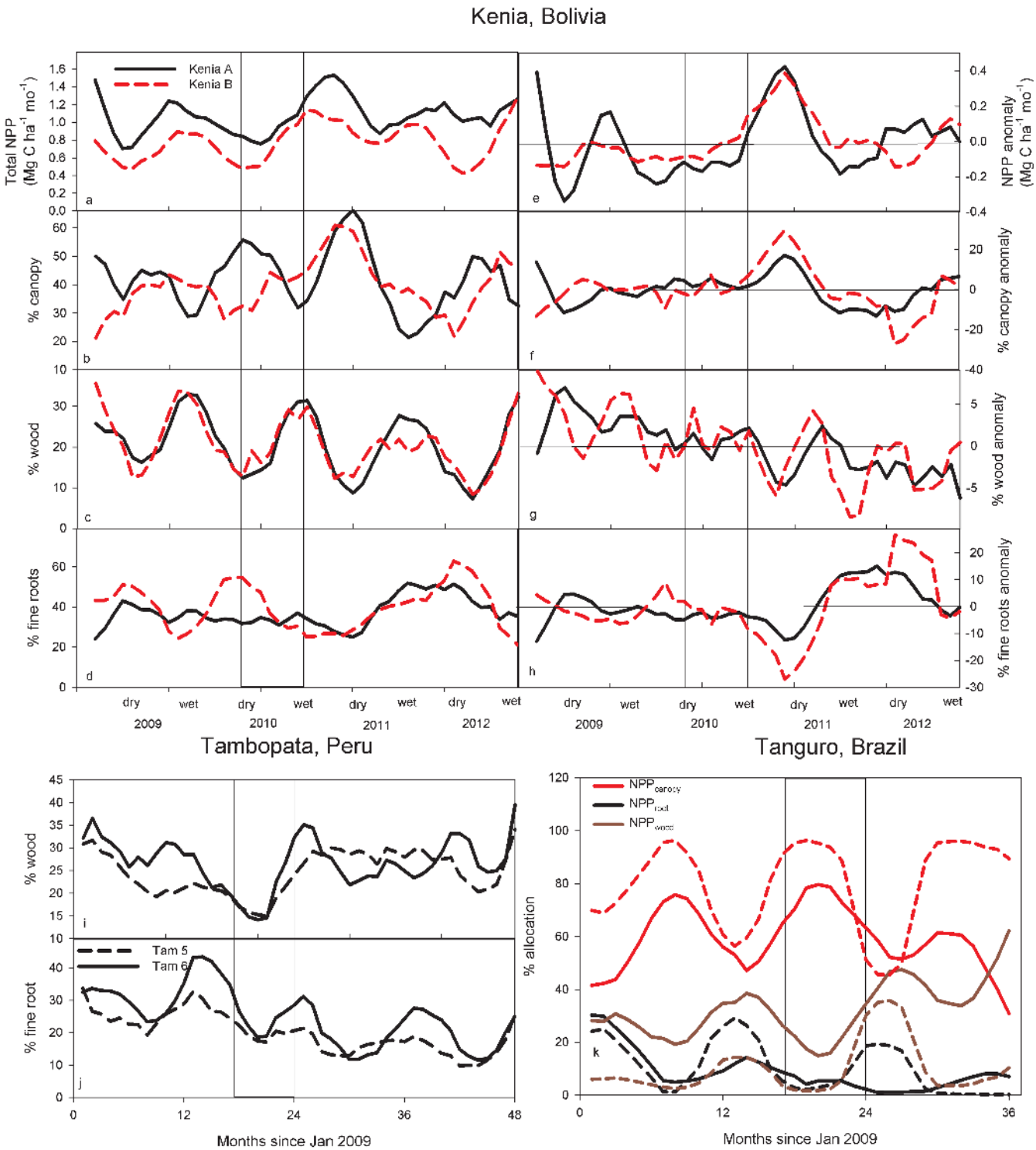

Extended Data Figure 5 | Impact of drought on carbon allocation for individual plots. This figure shows similar trends to those in Fig. 2, but with all the plots separated and extended for a further year for Tambopata and Kenia. **a**–**d**, Four years of total NPP (Mg C ha^{-1} per month) (**a**), percentage allocation to canopy (**b**), percentage allocation to wood (**c**) and percentage allocation to fine roots (**d**) for the two plots in Kenia, Bolivia (black line, Kenia-A; grey line, Kenia-B). **e**–**h**, Seasonally detrended anomaly data for the same variables. This data set is explored in detail in ref. 26. **i**, **j**, Comparison of four years of wood (**i**) and root (**j**) allocation data for two plots in Tambopata, Peru (black lines). Canopy NPP is not shown because LAI data were not processed for the entire 4-year period. **k**, Three years of woody (brown), fine-root (black) and canopy (red) allocation data for two plots in Tanguro, Brazil (solid line, Tanguro A; dashed line, Tanguro C). The bar indicates the approximate drought period.

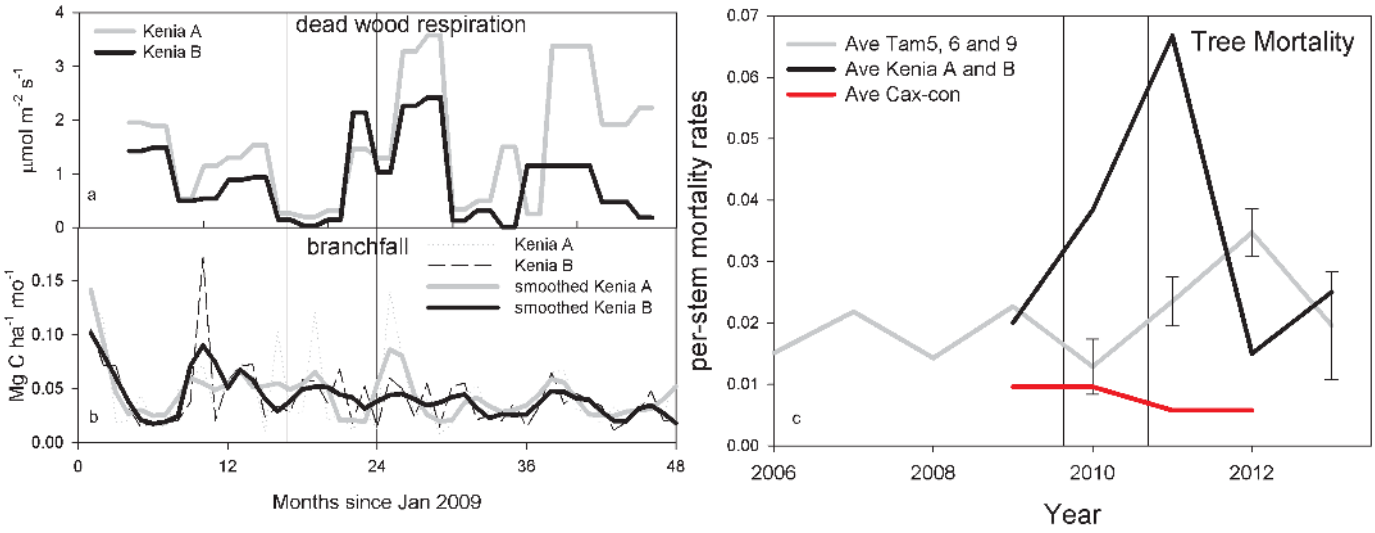

Extended Data Figure 6 | Deadwood respiration, branch fall and tree mortality. **a**, Respiration from deadwood over a 4-year period from Kenia-A (grey) and Kenia-B (black). **b**, Branch fall over a 4-year period from Kenia-A (grey) and Kenia-B (black); smoothed values are shown in bold lines; actual values are shown in dashed lines. **c**, Per-stem mortality rates for Peruvian drought plots (grey line, $n = 3$; error bars indicate standard errors), Bolivian drought plots (black line, $n = 2$) and the control plot in Caxiuanã (red line, $n = 1$). We do not show mortality for the Brazilian drought plots, but a recent paper[43] has shown an increase in mortality after drought at these sites. Mortality was marginally significantly higher ($P = 0.06$; paired 1-tailed t-test, $n = 5$) during the 2-year period after the drought than in other periods. The bar indicates the approximate period of the drought.

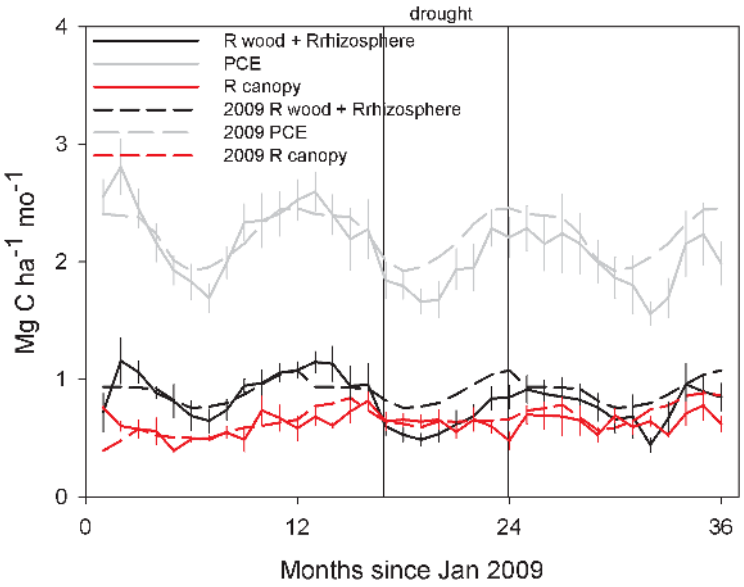

Extended Data Figure 7 | Separated components of PCE. Total PCE (grey solid line), wood and rhizosphere respiration (black solid line), and canopy respiration (red solid line) for the six droughted plots and smoothed 2009 equivalents (stippled lines). This figure shows that the decline in R_a was due to the components measured monthly (wood and rhizosphere respiration) and not to canopy respiration (which was measured only once or twice a year). This does not mean that canopy respiration did not decrease during the drought, only that we did not track canopy respiration sufficiently to measure changes. The bar indicates the approximate period of the drought.

Extended Data Table 1 | Methods for intensive monitoring of net primary production and photosynthesis

	Component	Description	Sampling period	Sampling interval
Net primary productivity (*NPP*)	Above-ground coarse wood net primary productivity (NPP_{ACW})	Forest inventory: All trees ≥ 10 cm DBH censused to determine growth rate of existing surviving trees and rate of recruitment of new trees, and identified floristically to derive wood density. Stem biomass calculated using the Chave et al. (2005) allometric equation for tropical moist forests, employing diameter, height and wood density data[44].	Kenia 2009-2013,Tambopata 2005-2013,Caxiuanã 2009-2010,Wayqecha 2009-2010,San Pedro 2009-2010,Tanguro 2009-2011	Every year (trees ≥ 10 cm DBH)
		Seasonal growth: Dendrometers were installed on most to all trees > 10cmDBH in each plot to determine the spatial-temporal and seasonal variation in growth.	Kenia 2009-2012,Tambopata 2009-2012,Caxiuanã 2009-2010,Wayqecha 2009-2010,San Pedro 2009-2010,Tanguro 2009-2011	Every month to 3 months
	Litterfall net primary productivity ($NPP_{litterfall}$)	Litterfall production of dead organic material less than 2 cm diameter was estimated by collecting litterfall in 0.25 m^2 (50 cm x 50 cm) litter traps placed at 1 m above the ground at the centre of each of the 25 subplots in each plot.	Kenia 2009-2012,Tambopata 2009-2012,Caxiuanã 2009-2010,Wayqecha 2009-2010,San Pedro 2009-2010,Tanguro 2009-2011	Every month
	Leaf area index (LAI)	Canopy images were recorded with a digital camera and hemispherical lens near the centre of each of the 25 subplots in each plot, at a standard height of 1 m during early morning or overcast conditions. LAI was estimated from these images using CAN-EYE software.	Kenia 2009-2012,Tambopata 2009-2012,Caxiuanã 2009-2010, Wayqecha 2009-2010,San Pedro 2009-2010,Tanguro 2009-2011	Every month
	Fine root net primary productivity ($NPP_{fine\ roots}$)	Sixteen ingrowth cores (mesh cages 14 cm diameter, installed to 30 cm depth) were installed in each plot. Cores were extracted and roots were manually removed from the soil samples in four 10 min time steps and the pattern of cumulative extraction over time was used to predict root extraction beyond 40 minutes. Root-free soil was then re-inserted into the ingrowth core. Collected roots were thoroughly rinsed, oven dried at 60°C to constant mass, and weighed.	Kenia 2009-2012,Tambopata 2009-2012,Caxiuanã 2009-2010,Wayqecha 2009-2010,San Pedro 2009-2010,Tanguro 2009-2011	Every 3 months
Leaf Photosynthesis	Saturated leaf photosynthesis (A_{sat})	Photosynthesis at PAR levels of 1000 µmol m^{-2} s^{-1}, 25°C temperature and ambient CO_2 concentrations (~400ppm) were recorded on ~20 trees per plot with an IRGA and specialized cuvette (Bolivia - Ciras 2, PPsystems, Tapajos – Licor 6400). In Bolivia, during the peak of the drought (November 2011) and again in June 2011, on the same trees during both periods, we randomly selected one branch each from the sunlit portion of the canopy and immediately re-cut the branches underwater to restore hydraulic connectivity. In the Tapajos, measurements were made weekly for 16 weeks on eight, top of canopy tree species accessed using canopy walk up towers (see Doughty 2011 for details)[41].	Kenia Nov 2010 and June 2011, and Tapajos, Brazil starting in June and measured weekly for 16 weeks	variable

See also the RAINFOR-GEM manual 2012 (available at http://gem.tropicalforests.ox.ac.uk/).

Extended Data Table 2 | Methods for intensive monitoring of autotrophic and heterotrophic respiration

	Component	Description	Sampling period	Sampling interval
R_a and R_h	Total soil CO_2 efflux (R_{soil})	Total soil CO_2 efflux was measured using a closed dynamic chamber method, at the centre of each of the 25 subplots in each plot with an infra-red gas analyser (IRGA; EGM-4) and soil respiration chamber (SRC-1) sealed to a permanent collar in the soil.	Kenia 2009-2012,Tambopata 2009-2012,Caxiuanã 2009-2010,Wayqecha 2009-2010,San Pedro 2009-2010,Tanguro 2009-2011	Every month
	Soil CO_2 efflux partitioned into autotrophic ($R_{rhizosphere}$) and heterotrophic ($R_{soilhet}$) components	At four points at each corner of the plot, we placed plastic tubes of 12 cm diameter; three tubes with short collars (10 cm depth) allowing both heterotrophic and rhizosphere respiration, three tubes with longer collars (40 cm depth) with no windows to exclude both roots and mycorrhizae. At the centre of each plot, a control experiment was carried out in order to assess the effects of root severing and soil structure disturbance that occurs during installation.	Kenia 2009-2012,Tambopata 2009-2012,Caxiuanã 2009-2010,Wayqecha 2009-2010,San Pedro 2009-2010,Tanguro 2009-2011	Every month
	Canopy respiration (R_{leaves})	In each plot, leaf dark respiration was recorded for an average of ~20 trees per plot with an IRGA and specialized cuvette. For each tree, we randomly selected one branch each from sunlit and shaded portions of the canopy and immediately re-cut the branches underwater to restore hydraulic connectivity. Leaves were placed in a black bag for at least 10 minutes prior to measurement.	Kenia 2010-2011,Tambopata 2010-2011,Caxiuanã 2007 Wayqecha 2010-2011,San Pedro 2010-2011	Once in dry season, once in wet season
	Above-ground live wood respiration (R_{stems})	Bole respiration was measured using a closed dynamic chamber method, from 25 trees distributed evenly throughout each plot at 1.3 m height with an IRGA (EGM-4) and soil respiration chamber (SRC-1) connected to a permanent collar, sealed to the tree bole surface.	Kenia 2009-2012,Tambopata 2009-2012,Caxiuanã 2009-2010,Wayqecha 2009-2010,San Pedro 2009-2010,Tanguro 2009-2011	Every 1-2 months
	Above-ground dead wood respiration	Representative samples of five decomposition categories of wood were placed in the respiration chamber (SRC-1) of an IRGA (EGM-4). See RAINFOR-GEM manual for description of decomposition status and surface area formulas to scale results to the 1 ha plot.	Kenia 2009-2012,Tambopata 2009-2012,Caxiuanã 2009-2010,Wayqecha 2009-2010,San Pedro 2009-2010,Tanguro 2009-2011	Every month to two months

See also the RAINFOR-GEM manual 2012 (available at http://gem.tropicalforests.ox.ac.uk/).

Extended Data Table 3 | Data analysis techniques for intensive study of carbon dynamics

	Component	Data processing details
Net primary productivity (NPP_{AG})	Above-ground coarse wood net primary productivity (NPP_{ACW})	Biomass calculated using the Chave *et al.* (2005)[39] allometric equation for tropical moist forests: $AGB = 0.0509 \times (\rho D^2 H)$ where AGB is aboveground biomass (kg), ρ is density (g cm^{-3}) of wood, D is dbh (cm), and H is (measured or if missing based on Feldpausch et al. 2012[36]) height (m). To convert biomass values into carbon, we assumed that dry stem biomass is 48-50% carbon based on the following reference[45].
	Branch turnover net primary productivity ($NPP_{branch\ turnover}$)	See RAINFOR-GEM manual for description of decomposition status and surface area formulas.
	Litterfall net primary productivity ($NPP_{litterfall}$)	Litterfall is separated into different components, oven dried at 60°C to constant mass and weighed. Litter is estimated to be 49.2% carbon, based on mean Amazonian values (S. Patiño, unpublished analysis).
	Leaf area index (LAI)	LAI was estimated using "true LAI" output from the Caneye program which accounts for clumping of foliage, and assumes a fixed leaf inclination angle, based on average estimates at individual plots. Leaves were separated into sunlit and shaded fractions using the following equation: $F_{sunlit} = (1-\exp(-K*LAI))/K$ where K is the light extinction coefficient, and F_{sunlit} is the sunlit leaf fraction[31]. The model assumptions are randomly distributed leaves, and $K = 0.5/\cos(Z)$ where Z is the solar zenith angle, which was set to 30° in this study.
	Fine root net primary productivity ($NPP_{fine\ roots}$)	Roots were manually removed from the soil samples in four 10 min time steps, according to a method that corrects for underestimation of biomass of hard-to-extract roots [46] and used to predict root extraction beyond 40 min (up to 100 minutes); we estimate that there was an additional 28% correction factor for fine roots not collected within 40 minutes. Correction for fine root productivity below 30 cm depth increased the value by 39%.
Autotrophic and heterotrophic respiration	Total soil CO_2 efflux (R_{soil})	Soil surface temperature (T260 probe, Testo Ltd, Hampshire, U.K.) and moisture (Hydrosense probe, Campbell Scientific Ltd, Loughborough, UK) were recorded at each point after efflux measurement.
	Soil CO_2 efflux partitioned into autotrophic ($R_{rhizosphere}$) and heterotrophic ($R_{soilhet}$) components	The partitioning experiment allows estimation of the relative contributions of (1) surface organic litter, (2) roots, (3) mycorrhizae and (4) soil organic matter to total soil CO_2 efflux. Contributions are estimated from differences between collars subjected to different treatments, in excess of pre-existing spatial variation.
	Canopy respiration (R_{leaves})	To scale to whole-canopy respiration, mean dark respiration for shade and sunlit leaves were multiplied by the respective estimated fractions of total LAI. To account for daytime light inhibition of leaf dark respiration, we apply the inhibition factor applied in Malhi *et al.* (2009) [47] (67% of daytime leaf dark respiration, 33% of total leaf dark respiration).
	Above-ground live wood respiration (R_{stems})	To estimate plot-level stem respiration tree respiration per unit bole area was multiplied by bole surface area (SA) for each tree, estimated with the following equation[48]: $\log(SA) = -0.105 - 0.686 \log(DBH) + 2.208 \log(DBH)^2 - 0.627 \log(DBH)^3$ Where DBH is bole diameter at 1.3 m height.

See also the RAINFOR-GEM manual 2012 (available at http://gem.tropicalforests.ox.ac.uk/).